NASA CONTRACTOR REPORT

NASA CR-2577

NASA CR-2577

TRANSONIC AIRFOIL FLOWFIELD ANALYSIS USING CARTESIAN COORDINATES

Leland A. Carlson

Prepared by
TEXAS A&M UNIVERSITY
College Station, Texas 77843
for Langley Research Center

NATIONAL AERONAUTICS AND SPACE ADMINISTRATION • WASHINGTON, D. C. • AUGUST 1975

1. Report No.	2. Government Accession No.	3. Recipient's Catalog No.
NASA CR-2577		

4. Title and Subtitle	5. Report Date
TRANSONIC AIRFOIL FLOWFIELD ANALYSIS USING CARTESIAN COORDINATES	AUGUST 1975
	6. Performing Organization Code

7. Author(s)	8. Performing Organization Report No.
Leland A. Carlson	
	10. Work Unit No.
	501-06-05-08-00
9. Performing Organization Name and Address	11. Contract or Grant No.
Texas A&M Research Foundation College Station, TX 77843	NGR-44-001-157
	13. Type of Report and Period Covered
12. Sponsoring Agency Name and Address	Contractor Report
National Aeronautics and Space Administration Washington, D. C.	14. Sponsoring Agency Code

15. Supplementary Notes

Monitored by Jerry C. South, Jr., Mail Stop 360
Langley Research Center, Hampton, VA 23665

FINAL REPORT

16. Abstract

A numerical technique for analyzing transonic airfoils is presented. The method employs the basic features of Jameson's iterative solution for the full potential equation, except that Cartesian coordinates are used rather than a grid which fits the airfoil, such as the conformal circle-plane or "sheared parabolic" coordinates that have been used previously. Comparison with previous results shows that it is not necessary to match the computational grid to the airfoil surface and that accurate results can be obtained with a Cartesian grid for lifting supercritical airfoils.

17. Key Words (Suggested by Author(s))	18. Distribution Statement
Supercritical Airfoil Analysis Relaxation Cartesian Coordinates	Unclassified-unlimited Subject Category 02

19. Security Classif. (of this report)	20. Security Classif. (of this page)	21. No. of Pages	22. Price*
Unclassified	Unclassified	33	$3.75

*For sale by the National Technical Information Service, Springfield, Virginia 22161

TRANSONIC AIRFOIL FLOWFIELD ANALYSIS USING CARTESIAN COORDINATES

By Leland A. Carlson
Texas A&M University

SUMMARY

A numerical technique for analyzing transonic airfoils is presented. The method employs the basic features of Jameson's iterative solution for the full potential equation, except that Cartesian coordinates are used rather than a grid which fits the airfoil, such as the conformal circle-plane or "sheared parabolic" coordinates that have been used previously. Comparison with previous results shows that it is not necessary to match the computational grid to the airfoil surface and that accurate results can be obtained with a Cartesian grid for lifting supercritical airfoils.

INTRODUCTION

The first practical numerical technique for solving two-dimensional steady transonic flows was developed by Murman and Cole [1] for the small perturbation equations in Cartesian coordinates. The essential features of this technique were the utilization of retarded (upwind) differences in regions of supersonic flow, central differences in subsonic zones, and the application of a far field boundary condition at a finite distance from the airfoil. The surface flow-tangency boundary condition was applied on the horizontal axis, consistent with the small disturbance approximation; and the resultant finite difference equations were solved iteratively by numerical relaxation. Shock waves occurred naturally in the course of solution as steep compressions smeared over several mesh points, and accurate results were obtained for slender airfoils.

This technique was subsequently extended to the complete potential flow equations and the exact boundary conditions by Garabedian and Korn [2], Steger and Lomax [3], and Jameson [4] and was successfully applied to thick, blunt-nosed, and aft-cambered airfoils. In these works the edge of the computational coordinate system was closely matched and aligned with the airfoil surface in order to accurately represent the surface flow-tangency boundary condition. For example, Steger and Lomax used a curvilinear wraparound system, while

Garabedian and Korn and also Jameson conformally mapped the exterior of the airfoil onto the interior of a unit circle with infinity corresponding to the circle origin. Jameson also used a parabolic type system [4] in another version designed to handle supersonic freestreams. These transformations had the advantage that near the body they aligned the coordinates with the flow, which is particularly advantageous in the leading edge region where body slopes and vertical velocities can be large. Unfortunately, such transformations introduce into the differential equation many, sometimes complicated, transformation derivatives.

Now in order for any backward difference scheme at supersonic points to work properly, the coordinate along which the backward differences are taken must be closely aligned with the flow direction. This alignment is very difficult to achieve with mapped coordinates when the freestream Mach number is high or the supersonic zone is large. On the other hand, improper alignment at supersonic points can lead to situations where the velocity component in each coordinate direction is subsonic, that is

$$U^2, V^2 < a^2 < U^2 + V^2 \tag{1}$$

This situation not only can lead to numerical instability but also can impart to the finite difference equations an incorrect zone of dependence. To remedy this problem South and Jameson [4,5] have introduced a rotated finite difference scheme which simulates a local rotation to coordinates along and normal to the velocity vector; and, in so doing, they have created a scheme that not only has the correct zone of dependence but also does not require coordinate alignment with the flow.

As a consequence of this development, the questions arose--Can the full potential flow equations be solved for a transonic case in a simple Cartesian or stretched Cartesian system by using the concept of rotated differences? If so, what is the accuracy and what are the properties of such an approach? In order to answer these questions, the present study was initiated. Its primary objectives have been

(a) To develop an analysis program using Cartesian coordinates (airfoil given, C_p and flowfield unknown)

(b) To develop a design program in Cartesian coordinates (C_p given, airfoil and flowfield unknown)

(c) To study the results obtained by such an approach and to determine the accuracy and idiosyncrasies associated with a Cartesian system.

This report describes the development of, and results obtained with, the analysis program. Reference 6 discusses the design program.

SYMBOLS

A_1, A_2, A_3	Coordinate stretching constants
a	isentropic speed of sound
a,b	coordinate stretching constants
C_p	pressure coefficient, $(p-p_\infty)/(\frac{1}{2}\rho_\infty U_\infty^2)$
C_L	lift coefficient
C_{MLE}	coefficient of moment about the leading edge
f,g	coordinate stretching functions
M	Mach number
N	coordinate normal to the streamwise direction
p	pressure
q	velocity
S	streamwise coordinate
t	time
U,V	velocity component in the x-,y- direction respectively
x,y	Cartesian coordinates
α	angle of attack or coefficient in Eq. (34)
β^2	$1-M_\infty^2$ or coefficient in Eq. (34)
γ	ratio of specific heats or coefficient in Eq. (34)
Γ	circulation
ε	damping coefficient
θ	polar coordinate
ξ,η	computational coordinates
ρ	density
Φ	potential function, Eq. (3)
ϕ	perturbation potential, Eq. (4)

Subscripts:

∞	freestream condition
b,body	body
TE	trailing edge
i,j	grid location
ξ,η,x,y	differentiation, i.e., $f_x = \frac{\partial f}{\partial x}$

Superscripts:

+	Value computed by current relaxation sweep

PROBLEM FORMULATION

The exact equation for the potential function for two dimensional compressible flow can be written in Cartesian coordinates as

$$(a^2 - \Phi_x^2)\Phi_{xx} - 2\Phi_x\Phi_y\Phi_{xy} + (a^2 - \Phi_y^2)\Phi_{yy} = 0 \tag{2}$$

where

$$\Phi_x = \frac{\partial \Phi}{\partial x}, \quad \Phi_{xx} = \frac{\partial^2 \Phi}{\partial x^2}, \quad \Phi_{xy} = \frac{\partial^2 \Phi}{\partial x \partial y} \quad \text{etc.}$$

If a perturbation potential, ϕ, is introduced such that

$$\Phi = xq_\infty \cos\alpha + yq_\infty \sin\alpha + q_\infty \phi \tag{3}$$

where the velocity components are given by

$$U = \Phi_x = q_\infty(\cos\alpha + \phi_x) \tag{4a}$$

$$V = \Phi_y = q_\infty(\sin\alpha + \phi_y) \tag{4b}$$

then the governing equation for the perturbation potential becomes

$$(a^2 - U^2)\phi_{xx} - 2UV\phi_{xy} + (a^2 - V^2)\phi_{yy} = 0 \tag{5}$$

with

$$a^2 = a_\infty^2 - \left(\frac{\gamma-1}{2}\right)[U^2 + V^2 - q_\infty^2] \tag{6}$$

The pressure coefficient at any point is given by

$$C_p = \frac{p - p_\infty}{\frac{1}{2}\rho_\infty U_\infty^2} = \frac{2}{\gamma M_\infty^2}\left\{\left[1 + \frac{\gamma-1}{2} M_\infty^2 \left(1 - \frac{U^2+V^2}{q_\infty^2}\right)\right]^{\frac{\gamma}{\gamma-1}} - 1\right\} \tag{7}$$

The appropriate boundary conditions are, at the airfoil surface

$$\left(\frac{dy}{dx}\right)_{body} = \left(\frac{V}{U}\right)_{body} \tag{8}$$

and at infinity [2,7,8]

$$\phi = \frac{-\Gamma}{2\pi} \text{ Tan}^{-1}(\beta \text{ Tan}(\theta - \alpha)) \tag{9}$$

where θ is the polar angle and Γ is the circulation determined by the change in potential across the Kutta-Joukowski cut at the trailing edge of the airfoil, i.e.

$$\Gamma = (\phi_{y=0^+} - \phi_{y=0^-})_{\text{Trailing Edge}} \tag{10}$$

NUMERICAL ANALYSIS

Coordinate Stretching

In the present problem an infinity boundary condition must be applied at the edge of the computational grid. It is convenient to transform or stretch the original x,y plane to some ξ,η plane so that the edges of the ξ,η grid correspond to infinity. In this way, Equation (9) can be applied directly. If this is not done, a far-field condition [8] can be used at the grid edges instead.

After investigating several possibilities, the coordinate stretching represented on Figure 1 was selected. Here x,y is the physical plane and ξ,η represents the computational plane, and each is subdivided into three regions. The stretching is symmetrical about the origin and it is given by

$$x = x_4 + A_2 \text{Tan}\left[\frac{\pi}{2}(\xi - \xi_4)\right] + A_3 \text{Tan}\left[\frac{\pi}{2}(\xi - \xi_4)^3\right] \tag{11}$$

in region III and by

$$x = \xi(a + b\,\xi^2) \tag{12}$$

in region II. The constants a and b are determined by the requirements

$$x = x_4 \quad \text{at} \quad \xi = \xi_4 \tag{13a}$$

and

$$\frac{dx}{d\xi} = \frac{\pi A_2}{2} \quad \text{at } \xi = \xi_4 \tag{13b}$$

The constant A_2 controls the grid spacing in the vicinity of x_4, usually near the leading and trailing edges; while A_3 determines the physical location of the grid line adjacent to the grid edge.

In the y-direction the stretching relationship is given by

$$y = A_1 \mathrm{Tan}\left(\frac{\pi}{2}\eta\right) \tag{14}$$

where A_1 controls the grid size near the airfoil.

Notice that the stretchings map the infinite physical x,y plane

$$-\infty \leq x \leq \infty$$
$$-\infty \leq y \leq \infty$$

into the finite computational plane

$$-(1 + \xi_4) \leq \xi \leq 1 + \xi_4$$
$$-1 \leq \eta \leq 1 \tag{15}$$

where ξ_4 determines the amount of the computational plane confined to the vicinity of the airfoil. A typical grid system is shown on Figure 2.

When selecting a stretching care must be taken to insure that the stretching does not force a physically unrealistic or abnormal behavior on the solution. For example, analysis of a compressible doublet indicates that ϕ_y and ϕ_x should decay as

$$\phi_y \sim \begin{cases} y^{-3} & \text{as } y \to \infty \\ x^{-3} & \text{as } x \to \infty \end{cases}$$

$$\phi_x \sim \begin{cases} x^{-2} & \text{as } x \to \infty \\ y^{-2} & \text{as } y \to \infty \end{cases} \tag{16}$$

In the present ξ,η system, this type of decay would require that

$$\phi_\eta \sim y^{-1} \text{ as } y \to \infty$$
$$\phi_\xi \sim \text{constant as } x \to \infty \tag{17}$$

and this type of behavior is quite permissible. However, with some other stretchings such as η=tanhy, the decay indicated by Equations (16) would require that

$$\phi_\eta \sim \infty \text{ as } y \to \infty,\ \eta \to 1 \tag{18}$$

In practice, it usually happens that the derivatives in the computational plane remain finite, even with the exponential stretchings; but this precludes the correct asympototic decay, and the effect may produce stable, convergent, wrong solutions.

Now as a result of the introduction of coordinate stretching, the governing equations should be written in terms of the independent computational variables ξ and η. By defining

$$f = \frac{d\xi}{dx}, \qquad g = \frac{d\eta}{dy} \tag{19}$$

Equations (4) and (5) become

$$(a^2 - U^2)f(f\phi_\xi)_\xi - 2UVfg\phi_{\xi\eta} + (a^2 - V^2)g(g\phi_\eta)_\eta = 0 \tag{20}$$

$$\begin{aligned} U &= q_\infty(\cos\alpha + f\phi_\xi) \\ V &= q_\infty(\sin\alpha + g\phi_\eta) \end{aligned} \tag{21}$$

Finite Difference Scheme

As indicated in the Introduction, in order to avoid at supersonic points difficulties associated with nonalignment of the coordinates and the flowfield a rotated finite difference scheme is used in the present problem. In this approach [4,5] the principal part of the governing differential equation can be written in coordinates parallel and perpendicular to the local velocity vector, S and N respectively, as

$$\left(1 - \frac{q^2}{a^2}\right)\phi_{SS} + \phi_{NN} = 0 \tag{22}$$

where

$$\phi_{SS} = \frac{1}{q^2}[U^2 f(f\phi_\xi)_\xi + 2UVfg\phi_{\xi\eta} + V^2 g(g\phi_\eta)_\eta]$$

$$\phi_{NN} = \frac{1}{q^2}[V^2 f(f\phi_\xi)_\xi - 2UVfg\phi_{\xi\eta} + U^2 g(g\phi_\eta)_\eta] \tag{23}$$

Notice that substitution of Equations (23) into (22) yields the governing equation, Eq. (20); and thus, as pointed out by South, [5] Eq. (22) is simply

a rearrangement of terms which exhibits the basic features of a local rotation to the streamline direction.

The basic concept [4,5] of the rotated scheme is to use, at supersonic points, first-order, upwind differencing in both the ξ and η directions for all contributions to ϕ_{SS} and central differencing for all contributions to ϕ_{NN}. In this manner the correct zone of dependence at supersonic points is built into the finite difference scheme. At subsonic points, the normal procedure of using central differences for all derivatives directly in Eq. (20) is used. Consequently, the scheme is second order accurate at subsonic points and first order accurate at supersonic points. The resulting finite difference equations are solved iteratively by using column relaxation sweeping from upstream to downstream. In such a procedure the values obtained during an iterative sweep can be thought of as new values, ϕ^+_{ij}; while those obtained during the previous sweep can be considered old values, ϕ_{ij}. In this manner, the change from one iteration to the next can be viewed as that occurring during some artificial time step, Δt; and artificial time derivatives such as ϕ_t, $\phi_{\xi t}$ and $\phi_{\eta t}$ can be considered. Of course, as the relaxation process converges, these terms become negligible.

Various investigators have used different finite difference formulas to represent the derivatives in Eq. (23). For example, Jameson [4] and South and Jameson [5] used in their finite difference formulation a mixture of old and new values. In this way, terms such as ϕ_{St} and ϕ_{Nt} were implicitly added to the problem and used to control numerical stability. Since it was determined by Jameson [4] that additional ϕ_{St} needed to be explicitly added to the problem in order to insure stability, it was decided in the present case to use all old values in the difference expressions for ϕ_{SS} and to add ϕ_{St} explicitly. For ϕ_{NN}, appropriate combinations of old and new values were used, causing ϕ_{Nt} to occur implicitly. It should be emphasized again that ϕ_{Nt} and ϕ_{St} go to zero as the solution converges, and hence do not affect the final result.

Thus the finite difference expressions used in the present formulation are:

For contributions to ϕ_{NN} when $q^2 > a^2$

$$(f\phi_\xi)_\xi = \frac{1}{\Delta\xi^2}\{f_{i+\frac{1}{2}}(\phi_{i+1,j} - \phi_{ij}) - f_{i-\frac{1}{2}}(\phi^+_{ij} - \phi^+_{i-1,j})\} \tag{24a}$$

$$\phi_{\xi\eta} = \frac{1}{4\Delta\xi\Delta\eta}\{\phi^+_{i-1,j} - \phi^+_{i-1,j+1} - \phi_{i+1,j-1} + \phi_{i+1,j+1}\} \tag{24b}$$

$$(g\phi_\eta)_\eta = \frac{1}{\Delta\eta^2}\{g_{j+\frac{1}{2}}(\phi^+_{i,j+1} - \phi^+_{ij}) - g_{j-\frac{1}{2}}(\phi^+_{ij} - \phi^+_{i,j-1})\} \tag{24c}$$

For contributions to ϕ_{SS} when $q^2 > a^2$ and $V > 0$

$$(f\phi_\xi)_\xi = \frac{1}{\Delta\xi^2}\{f_{i-\frac{1}{2}}(\phi_{ij} - \phi_{i-1,j}) - f_{i-3/2}(\phi_{i-1,j} - \phi_{i-2,j})\} \tag{25a}$$

$$\phi_{\xi\eta} = \frac{1}{\Delta\xi\Delta\eta}\{\phi_{ij} - \phi_{i-1,j} - \phi_{i,j-1} + \phi_{i-1,j-1}\} \tag{25b}$$

$$(g\phi_\eta)_\eta = \frac{1}{\Delta\eta^2}\{g_{j-\frac{1}{2}}(\phi_{ij} - \phi_{i,j-1}) - g_{j-3/2}(\phi_{i,j-1} - \phi_{i,j-2})\} \tag{25c}$$

where to create stability there is added to the basic equation

$$-\frac{\varepsilon\Delta t}{\Delta\xi} f\phi_{S_t} = -\frac{\varepsilon f\Delta t}{\Delta\xi}\left[\frac{Uf}{q}\phi_{\xi t} + \frac{Vg}{q}\phi_{\eta t}\right]$$

$$= -\frac{\varepsilon f}{\Delta\xi}\left[\frac{Uf_{i-\frac{1}{2}}}{\Delta\xi q}(\phi^+_{ij} - \phi_{ij} - \phi^+_{i-1,j} + \phi_{i-1,j})\right.$$

$$\left. + \frac{V}{q}\frac{g_{j-\frac{1}{2}}}{\Delta\eta}(\phi^+_{ij} - \phi_{ij} - \phi^+_{i,j-1} + \phi_{i,j-1})\right] \tag{25d}$$

For contributions to ϕ_{SS} when $q^2 > a^2$ and $V < 0$

$$(f\phi_\xi)_\xi = \frac{1}{\Delta\xi^2}\{f_{i-\frac{1}{2}}(\phi_{ij} - \phi_{i-1,j}) - f_{i-3/2}(\phi_{i-1,j} - \phi_{i-2,j})\} \tag{26a}$$

$$\phi_{\xi\eta} = \frac{1}{\Delta\xi\Delta\eta}\{-\phi_{ij} + \phi_{i-1,j} + \phi_{i,j+1} - \phi_{i-1,j+1}\} \tag{26b}$$

$$(g\phi_\eta)_\eta = \frac{1}{\Delta\eta^2}\{g_{j+\frac{1}{2}}(\phi_{ij} - \phi_{i,j+1}) - g_{j+3/2}(\phi_{i,j+1} - \phi_{i,j+2})\} \tag{26c}$$

and to create stability there is added

$$-\frac{\varepsilon f\Delta t}{\Delta\xi}\phi_{St} = -\frac{\varepsilon f}{\Delta\xi}\left[\frac{U}{q}\frac{f_{i-\frac{1}{2}}}{\Delta\xi}(\phi^+_{ij} - \phi_{ij} - \phi^+_{i-1,j} + \phi_{i-1,j})\right.$$

$$\left. + \frac{V}{q}\frac{g_{j+\frac{1}{2}}}{\Delta\eta}(-\phi^+_{ij} + \phi_{ij} + \phi^+_{i,j+1} - \phi_{i,j+1})\right] \tag{26d}$$

At points where $q^2 < a^2$ the expressions are

$$(f\phi_\xi)_\xi = \frac{1}{\Delta\xi^2}\{f_{i+\frac{1}{2}}\phi_{i+1,j} - (f_{i+\frac{1}{2}} + f_{i-\frac{1}{2}})[\frac{\phi^+_{ij}}{w} + (1-\frac{1}{w})\phi_{ij}] + f_{i-\frac{1}{2}}\phi^+_{i-1,j}\} \tag{27a}$$

$$\phi_{\xi\eta} = \frac{1}{4\Delta\xi\Delta\eta}\{\phi^+_{i-1,j-1} - \phi^+_{i-1,j+1} - \phi_{i+1,j-1} - \phi_{i+1,j+1}\} \tag{27b}$$

$$(g\phi_\eta)_\eta = \frac{1}{\Delta\eta^2}\{g_{j+\frac{1}{2}}(\phi^+_{i,j+1} - \phi^+_{ij}) - g_{j-\frac{1}{2}}(\phi^+_{ij} - \phi^+_{i,j-1})\} \tag{27c}$$

where the relaxation factor, w, has been incorporated into the difference formulas.

In all cases the velocities, U and V, are represented by central differences using old values. When these expressions, Eqs. (24) to (27), are substituted appropriately into Eqs. (22) and (23) or Eq. (20), the result is a tridiagonal system of equations that can be solved for the values of ϕ^+_{ij} on column i.

Treatment of Boundary Conditions

There are many ways to approximate the flow tangency condition, Eq. (8), at the airfoil boundary. One of the simplest, which is used here, is to generate dummy values of ϕ at mesh points inside the boundary such that the usual difference equations can be solved at points just outside the boundary. The problem is to develop a scheme for providing and updating these dummy values by using the surface flow tangency condition and neighboring values of ϕ in the mesh, with adequate accuracy and without creating instability.

To accomplish this, we first note that, in the computational coordinates, Eq. (8) becomes:

$$(\frac{dy}{dx})_b = \frac{V_b}{U_b} = \frac{\sin\alpha + g_b\phi_{\eta b}}{\cos\alpha + f_b\phi_{\xi b}} \tag{28}$$

Next a Taylor series about the dummy point (i,j-1) is written (see figure 3):

$$\phi_{\eta_b} = \phi_{\eta_{i,j-1}} + (\eta_b - \eta_{j-1})\phi_{\eta\eta_{i,j-1}} + \ldots \tag{29a}$$

$$\phi_{\xi_b} = \phi_{\xi_{i,j-1}} + (\eta_b - \eta_{j-1})\phi_{\xi\eta_{i,j-1}} + \ldots \tag{29b}$$

When these are written in finite difference form using second order expressions for ϕ_ξ and ϕ_η and at least first order ones for $\phi_{\eta\eta}$ and $\phi_{\xi\eta}$ they become (for the upper surface case)

$$\phi_{\eta_b} = \frac{-3\phi_{i,j-1} + 4\phi_{ij} - \phi_{i,j+1}}{2\Delta\eta}$$

$$+(\eta_b - \eta_{j-1})\left(\frac{\phi_{i,j-1} - 2\phi_{ij} + \phi_{i,j+1}}{\Delta\eta^2}\right) \qquad (30a)$$

$$\phi_{\xi_b} = \frac{\phi_{i+1,j-1} - \phi_{i-1,j-1}}{2\Delta\xi}$$

$$+(\eta_b - \eta_{j-1})\left(\frac{\phi_{i+1,j} - \phi_{i+1,j-1} - \phi_{i-1,j} + \phi_{i-1,j-1}}{2\Delta\xi\Delta\eta}\right) \qquad (30b)$$

These expressions can then be substituted into Eq. (28) and the result solved for a sufficiently accurate $\phi_{i,j-1}$ that is in terms of the neighboring potentials, body slope, and body position.

For those situations where the flow at point (i,j) is supersonic and $V_{ij} > 0$ examination of Eqs. (25) show that the difference scheme will require a $\phi_{i,j-2}$ value as well as $\phi_{i,j-1}$. Thus, in all cases a value of $\phi_{i,j-2}$ is determined by extrapolation as

$$\phi_{i,j-2} = -\phi_{ij} + 2\phi_{i,j-1} \qquad (31)$$

The above procedure for determining the values of the dummy mesh points inside the boundary is performed twice for the relaxation procedure of column i. First, Eq. (28) is used with ϕ values obtained by the previous relaxation sweep in order to obtain old values for the dummy points $\phi_{i,j-1}$ and $\phi_{i,j-2}$. Then, after column i has been relaxed, it is used again with as many current values of ϕ as possible to obtain new values $\phi^+_{i,j-1}$ and $\phi^+_{i,j-2}$. In this manner, the dummy mesh points will have both old and new values just like regular mesh points, and they can be used directly in the finite difference formulas without special treatment.

A similar procedure is used to satisfy the boundary conditions on the lower surface of the airfoil.

At the edge of the grid the infinity boundary condition given by Eq. (9)

must be used. In the stretched ξ,η system the polar angle will have at the edge of the grid the values shown on Figure 4. Thus, the boundary values will be

On line AB, $\theta = 0$, $\phi = \frac{-\Gamma}{2\pi}(-\text{Tan}^{-1}(\beta\text{Tan}\alpha))$ (32a)

On line BC, $\theta = \frac{\pi}{2}$, $\phi = \frac{-\Gamma}{2\pi}\ \text{Tan}^{-1}(\beta\cot\alpha)$ (32b)

On line CD, $\theta = \pi$, $\phi = \frac{-\Gamma}{2\pi}(\pi - \text{Tan}^{-1}(\beta\text{Tan}\alpha))$ (32c)

On line DE, $\theta = \frac{3\pi}{2}$, $\phi = \frac{-\Gamma}{2\pi}(\pi + \text{Tan}^{-1}(\beta\cot\alpha))$ (32d)

On line EF, $\theta = 2\pi$, $\phi = \frac{-\Gamma}{2\pi}(2\pi - \text{Tan}^{-1}(\beta\text{Tan}\alpha))$ (32e)

Boundary values must also be assigned to the singular corner points B, C, D, and E since they will be used in the finite difference formula for $\phi_{\xi\eta}$. The choice of these values is somewhat arbitrary since they depend upon how the corner points are approached. Fortunately, numerical studies indicate that the solution is insensitive to the values selected; and, thus, the following have been used.

Point B, $\phi = \frac{-\Gamma}{2\pi}\ \text{Tan}^{-1}\left(\frac{A_1}{A_2}\ \frac{\Delta\xi}{\Delta\eta}\right)$ (33a)

Point C, $\phi = \frac{-\Gamma}{2\pi}\left(\pi - \text{Tan}^{-1}\left(\frac{A_1}{A_2}\ \frac{\Delta\xi}{\Delta\eta}\right)\right)$ (33b)

Point D, $\phi = \frac{-\Gamma}{2\pi}\left(\pi + \text{Tan}^{-1}\left(\frac{A_1}{A_2}\ \frac{\Delta\xi}{\Delta\eta}\right)\right)$ (33c)

Point E, $\phi = \frac{-\Gamma}{2\pi}\left(2\pi - \text{Tan}^{-1}\left(\frac{A_1}{A_2}\ \frac{\Delta\xi}{\Delta\eta}\right)\right)$ (33d)

These assume that the corner points are approached along a diagonal (in the ξ-η plane) connecting the interior point just inside the corner and the corner points.

Using the above finite difference formulas and boundary conditions, the governing differential equation can be solved iteratively by column relaxation. For each iteration, the sweep pattern is from upstream to downstream in the region in front of the airfoil, then in the region above the airfoil, then below the airfoil, and finally in the portion downstream of the trailing edge. The latter region contains the Kutta-Joukowski cut, and the equations are appropriately differenced to give the proper jump in the potential.

NUMERICAL STABILITY

Supersonic Points

The incorporation into the finite difference formulas of both old, ϕ, and new, ϕ^+, values and the explicit inclusion of ϕ_{St} at supersonic points introduces time-like derivatives into the equation being solved. Thus, during the iterative process the actual equation at supersonic points is of the form

$$\gamma\phi_t + \left(\frac{q^2}{a^2} - 1\right)\phi_{SS} + 2\alpha\phi_{St} - \phi_{NN} + 2\beta\phi_{Nt} = 0 \tag{34}$$

Jameson [4] has shown that for numerical stability the coefficients must be such that

$$\gamma = 0 \tag{35a}$$

$$\alpha^2 > \beta^2\left(\frac{q^2}{a^2} - 1\right) \tag{35b}$$

In the present problem, a proper value for ε can be determined from Eq. (35b) once α and β are determined. Since the ϕ_{St} is included explicitly (see Eqs. (25d) and (26d)), the α is known, and the β can be determined from the ϕ_{NN} term.

By adding and subtracting old values of ϕ to get ϕ_{NN} in terms of old values, the time-like derivatives can be isolated. Thus

$$\begin{aligned}\phi_{NN} - 2\beta\phi_{Nt} = \phi_{NN} + {} & \frac{V^2 f}{q^2}\left[\frac{-f_{i-\frac{1}{2}}\left(\phi^+_{ij} - \phi_{ij}\right)}{\Delta\xi^2} + f_{i-\frac{1}{2}}\,\frac{\left(\phi^+_{i-1,j} - \phi_{i-1,j}\right)}{\Delta\xi^2}\right] \\ & -\frac{2UVfg}{q^2}\left[\frac{\phi^+_{i-1,j-1} - \phi_{i-1,j-1} - \phi^+_{i-1,j+1} + \phi_{i-1,j+1}}{4\Delta\xi\Delta\eta}\right] \\ & +\frac{U^2 g}{q^2}\left[g_{j+\frac{1}{2}}\,\frac{\left(\phi^+_{i,j+1} - \phi_{i,j+1} - \phi^+_{ij} + \phi_{ij}\right)}{\Delta\eta^2}\right. \\ & \left. -g_{j-\frac{1}{2}}\,\frac{\left(\phi^+_{ij} - \phi_{ij} - \phi^+_{i,j-1} + \phi_{i,j-1}\right)}{\Delta\eta^2}\right]\end{aligned} \tag{36}$$

$$= \phi_{NN} - \frac{V^2 f}{q^2} \frac{\Delta t}{\Delta \xi} (f\phi_{\xi t})_{i-\frac{1}{2},j} + \frac{UVfg}{q^2} \frac{\Delta t}{\Delta \xi} (\phi_{\eta t})_{i-1,j}$$

$$+ \frac{Ug^2}{q^2} \frac{\Delta t}{\Delta \eta} [(g\phi_{\eta t})_{i,j+\frac{1}{2}} - (g\phi_{\eta t})_{i,j-\frac{1}{2}}] \qquad (36)$$

which in the limit of vanishing step size becomes

$$\phi_{NN} - 2\beta\phi_{Nt} = \phi_{NN} + \frac{Vf}{q} \frac{\Delta t}{\Delta \xi} \left[\frac{-V}{q} f\phi_{\xi t} + \frac{Ug}{q} \phi_{\eta t} \right] \qquad (37)$$

where the term in brackets is ϕ_{Nt}. Hence, from a time-like viewpoint the actual differential equation being solved is

$$\left(1 - \frac{q^2}{a^2}\right) \phi_{SS} - \frac{\varepsilon \Delta t}{\Delta \xi} f\phi_{St} + \phi_{NN} + \frac{V}{q} \frac{f}{\Delta \xi} \Delta t \, \phi_{Nt} = 0 \qquad (38)$$

and so

$$\gamma = 0$$

$$\alpha = \frac{\varepsilon \Delta t f}{2\Delta \xi} \qquad \beta = \frac{-Vf\Delta t}{q\Delta \xi} \qquad (39)$$

Thus, from Eq. (35), a necessary condition for stability is

$$\varepsilon^2 > \frac{V^2}{q^2} \left(\frac{q^2}{a^2} - 1 \right) \qquad (40)$$

Notice that this requirement means that, for a fixed value for ε, numerical instability is most likely to occur where the local Mach number is large, say immediately upstream of a shock wave. Numerical experiments have been conducted to verify Eq. (40), and in most cases instability, if present, does originate from the high Mach number region in front of a shock wave. However, the minimum value of ε predicted by Eq. (40) is usually much smaller than the value actually required in practice. This latter phenomena has also been observed by other investigators using time-like damping, and usually the actual value is only slightly less than ε_{max} where

$$\varepsilon_{max}^2 \sim M_{max}^2 - 1 \qquad (41)$$

Subsonic Damping

Since at subsonic points Eq. (20) is used while at supersonic points Eq. (22) is solved, there is the possibility that during the initial iterative stages that the time dependent terms of the two finite difference equation forms do not match near the sonic line. This mismatch possibility can be prevented by adding to the subsonic finite difference equation a term

$$-\frac{\varepsilon\Delta tf}{\Delta\xi}\,\phi_{St} = -\frac{\varepsilon\Delta tf}{\Delta\xi}\left[\frac{Uf}{q}\,\phi_{\xi t} + \frac{V}{q}\,g\,\phi_{\eta t}\right] \tag{42}$$

which when q equals a causes the supersonic and subsonic difference equations to match exactly.

The question naturally arises, however, of what effect does Eq. (42) have upon convergence and stability away from sonic points. By substituting Eqs. (27) into Eq. (20) and isolating the time-like terms, it can be determined that the actual equation being solved at subsonic points is

$$\begin{aligned}&\left(1-\frac{U^2}{a^2}\right) f\,(f\phi_\xi)_\xi - \frac{2UV}{a^2}\,fg\phi_{\xi\eta} + \left(1-\frac{V^2}{a^2}\right) g\,(g\phi_\eta)_\eta \\ &+ \left(1-\frac{U^2}{a^2}\right)\frac{f^2\Delta t}{\Delta\xi^2}\left(\frac{w-2}{w}\right)\phi_t - \left(1-\frac{U^2}{a^2}\right)\frac{f^2}{\Delta\xi}\,\Delta t\phi_{\xi t} \\ &+ \frac{UVfg}{a^2}\,\frac{\Delta t}{\Delta\xi}\,\phi_{\eta t} - \varepsilon\,\frac{\Delta tf}{\Delta\xi}\left[\frac{Uf}{q}\,\phi_{\xi t} + \frac{V}{q}\,g\phi_{\eta t}\right] = 0\end{aligned} \tag{43}$$

Far away from the supersonic zone and the airfoil, V will normally be very small and the effective equation will be

$$\begin{aligned}&\left(1-\frac{U^2}{a^2}\right) f\,(f\phi_\xi)_\xi + g\,(g\phi_\eta)_\eta + \left(1-\frac{U^2}{a^2}\right)\frac{f^2}{\Delta\xi^2}\,\Delta t\left(\frac{w-2}{w}\right)\phi_t \\ &- \left[\left(1-\frac{U^2}{a^2}\right)\frac{f^2\Delta t}{\Delta\xi} + \frac{\varepsilon\Delta tf}{\Delta\xi}\,\frac{Uf}{q}\right]\phi_{\xi t} = 0\end{aligned} \tag{44}$$

In order to see the effect of the $\varepsilon\phi_{\xi t}$ term on the solution behavior of this equation assume

$$\begin{aligned} f &\approx g \\ \Delta t &\approx \Delta\xi \\ U &\approx q \end{aligned} \tag{45}$$

and let

$$A = 1 - \frac{U^2}{a^2} \approx \text{constant} \tag{46}$$

Then Eq. (44) can be modeled as

$$A\phi_{\xi\xi} + \phi_{\eta\eta} = \frac{A}{\Delta\xi}\left(\frac{2 - w}{w}\right)\phi_t + A\phi_{\xi t} + \varepsilon\phi_{\xi t} \tag{47}$$

The convergence behavior of this equation can be studied following the approach of Garabedian [9]. First, transform from (ξ,η,t) to (ξ,η,s) by

$$s = t + \left(\frac{A + \varepsilon}{2A}\right)\xi \tag{48}$$

and assume solution of the form $\phi = U(\xi,\eta)W(s)$.
Thus, in general, the solution to Eq. (47) is

$$\phi = U_0(\xi,\eta) + \sum_{m=1}^{\infty} W_m U_m \tag{49}$$

where W_m and U_m are eigenfunctions and

$$W_m = C_m e^{p_{m1}s} + D_m e^{p_{m2}s} \tag{50}$$

and

$$p_{m_{1,2}} = \frac{-\beta \pm \left[\beta^2 - 4\alpha Km^2\right]^{\frac{1}{2}}}{2\alpha} \tag{51}$$

and C_m and D_m are the Fourier coefficients.

Obviously, the rate of decay of the time terms is determined by the real part of P_{11}, and the optimum convergence rate will occur when the relaxation factor, w, is such that the radical in Eq. (51) is zero. When it is zero or pure imaginary, the rate of convergence will be determined by

$$p = \frac{-\beta}{2\alpha} = \frac{-2A^2\left(\frac{2 - w}{w}\right)}{\Delta\xi\ (A + \varepsilon)^2} \tag{52}$$

For a fixed relaxation factor, as the damping coefficient, ε, increases, the radical in Eq. (51) eventually goes negative; and the error, E, due to N relaxation iterations will be of the order

$$E = O\left(e^{-pN\Delta t}\right) \tag{53}$$

Since p decreases as $(A + \varepsilon)^{-2}$, an increase in ε from zero to one can cause an order of magnitude increase in the number of iterations required for convergence.

From this analysis it can be concluded that the addition of $\varepsilon\phi_{St}$ at subsonic points decreases significantly the rate of convergence and that large values of ε should be avoided.

In addition, South has shown by a linear stability analysis that for the model equation

$$\phi_{xx} + \phi_{yy} - \varepsilon U\phi_{xt} - \varepsilon V\phi_{yt} = 0 \tag{54}$$

that the inclusion of explicit time-like damping in addition to that implicitly obtained by the finite difference forms of ϕ_{xx} and ϕ_{yy} can, in a stretched coordinate system, be destabilizing and may cause numerical instability, particularly in regions of hard stretching where V is large.

Based upon these two analyses, both of which have been verified numerically, it is believed the specific addition of $\varepsilon\phi_{St}$ at subsonic points should be avoided and that the mismatch in time-like terms near sonic points should be prevented by changing the damping coefficient at supersonic points to $[M^2 - 1]^{\frac{1}{2}}\varepsilon$.

NUMERICAL STUDIES

In actually carrying out the numerical solution the parameters A_1, A_2, and A_3, should be selected so that the grid spacing Δx and Δy is small near the airfoil, and x_4 should be near the trailing edge. The question is How small and How close? See Figure 5.

To answer these questions a series of numerical experiments were conducted and it was determined that accurate results for lift and surface pressures could be obtained when

$$\frac{\Delta x}{c} \simeq \frac{\Delta y}{c} \simeq \frac{2r_{LE}}{c} \tag{55}$$

in the vicinity of the leading edge. (In the present computer formulation the chord c is always unity. The airfoil leading edge is at x = -0.5 and the trailing edge at x = +0.5.) No significant changes in lift or surface pressures were observed for smaller step sizes as long as Δx was about the same

magnitude as Δy near the leading edge. However, when Δy was three times Δx near the leading edge good accuracy was not acheived until

$$\frac{\Delta x}{c} \sim \frac{r_{LE}}{c} \quad , \quad \Delta y \sim 3\Delta x \tag{56}$$

and considerable sensitivity to the value of Δx was observed. In addition, the pressure coefficient near the nose exhibited slight oscillatory behavior.

Considerable sensitivity was also observed for the value chosen for x_4, which essentially determines the first and last grid points on the airfoil. For a grid spacing given by Eq. (55), x_4 values of 0.50 and 0.49 yielded pressure coefficient results that differed by as much as ten percent, with the results associated with the 0.5 value being worse. In addition, sensitivity to grid spacing was observed in the 0.5 case but was minimal in the 0.49 case. Further investigation showed that if the spacing near the leading edge were reduced to r/c, either by using more points or by coordinate stretching, that good results insensitive to the x_4 choice could be obtained even for x_4 values near 0.5. The cause of this behavior is not at present completely understood.

Based upon these results and those previously discussed concerning numerical stability, it is believed that accurate solutions can be obtained when

$$X_4 \simeq 0.49 \leftrightarrow 0.495$$

$$\frac{\Delta x}{c} \simeq \frac{\Delta y}{c} \simeq \frac{2r_{LE}}{c} \qquad \text{near the leading edge} \tag{57}$$

In addition, considering the destabilizing effects of hard stretching, it is recommended that whenever possible Δx be kept relatively constant between the leading and trailing edges of the airfoil.

COMPARISONS AND TYPICAL RESULTS

Any new numerical technique can only be verified by comparing its results with those previously obtained by other investigators. As suggested by Lock, [10] the NACA 0012 airfoil is an excellent test case because its shape can be exactly prescribed analytically; and the solutions of Sells, [11] which are believed to have an accuracy to about 1%, can be used for comparison for subcritical cases.

Figure 6 compares the results obtained by the present method with those of Sells for a nonlifting subcritical case. As can be seen the two pressure distributions agree exactly with the exception of the immediate vicinity of the trailing edge. The latter small disagreement may be due to the fact that in the Sells case the airfoil is extended 0.89% to yield zero trailing edge thickness while in the present case it is not. Also, in the present case the symmetry present in the nonlifting flow is not imposed, and the circulation is actually a calculated zero.

Pressure distribution results for a lifting subcritical NACA 0012 flow are shown on Figure 7 and again the results are compared with those obtained using the Sells method. [10] Here, the two sets of data are always within two percent of each other and the lift coefficients agree exactly. In particular, notice the excellent agreement on the magnitude and location of the upper surface pressure peak.

The above cases are excellent for validating the present Cartesian coordinate solution on airfoils having large leading edge radii. However, many airfoils of practical interest have very small leading edge radii and extremly rapid upper surface expansion near the leading edge. For example, the NACA 63A006 airfoil has a leading edge radius only one-sixth that of the NACA 0012. Results for this airfoil at M_∞ of 0.6 and an angle of attack of two degrees are shown on Figure 8. The present solution was obtained with a medium sized grid of 49 by 49, which yielded 66 points on the airfoil surfaces. Superimposed on this pressure distribution is a result obtained by Newman at NASA Langley using a program developed by Jameson. This Jameson program, which uses conformal coordinates in the circle plane, is believed to be very accurate at both subcritical and supercritical speeds, and the results shown on Figure 8 were obtained with a 192 x 32 grid with 192 points on the airfoil surfaces. While the Cartesian grid had insufficient points to completely resolve the very sharp pressure peak, the C_p values at given x locations agree with those by Jameson at the same x locations. In addition, the concavity variations in the upper surface pressure coefficient distribution are accurately reproduced; and the computed lift and moment coefficients agree within less than two percent.

Based upon the comparisons shown on Figures 6-8, it is believed that for subcritical cases the present Cartesian system method can yield accurate

results using medium-sized computational grids. For supercritical cases, comparison and verification is somewhat more difficult. However, comparison with results obtained by Jameson's program for an analytically defined airfoil, such as an NACA 0012, should suffice.

Figure 9 shows such a comparison for an NACA 0012 at a freestream Mach number of 0.75 and two degree angle of attack. Again the lift and moment coefficients essentially agree exactly, and the pressure coefficients and shock location agree quite well. The present results do show a slight re-expansion immediately downstream of the shock wave that becomes more pronounced with further reduction in grid spacing. It is believed that this expansion is detected because for this case the Cartesian grid is better aligned with the shock that the conformal grid.

These comparisons demonstrate that accurate transonic flow solutions can be obtained in a Cartesian grid system. Further, they show that there is little loss of accuracy associated with not mapping the computational grid to match the airfoil surface and that excellent results can be efficiently obtained using only medium grids.

In addition to the above comparison cases, the present analysis program has been applied to many airfoils specifically designed for transonic flight. For example, Figure 10 shows the pressure distribution obtained by the present method for an aft-cambered supercritical airfoil. This airfoil was designed [6] with a leading edge radius of 0.0245c and a weak shock (upstream Mach number of about 1.20) near the three-quarter chord point, in accordance with the design criteria advocated by Whitcomb. [12] The airfoil shape portrayed on Figure 10 is not the actual surface but the displacement surface, and a preliminary analysis indicates that the boundary layer is free from separation effects.

Figure 11 shows the result of a direct analysis with the present program of an entirely different type of supercritical airfoil. This airfoil was designed [6] to have the same basic lift coefficient and lower surface pressure distribution as that of an NACA 0012 and the moment coefficient was to be lower than that of an aft-cambered airfoil. As can be seen from the present direct analysis, these objectives were essentially achieved, although the lift coefficient is slightly higher. Again, the airfoil shape portrayed is the

displacement surface, and it has a $(t/c)_{max}$ of 0.1265 at the 0.3753 chord point with a leading edge radius of 0.0146.

The results shown on Figures 6 to 11 were typically obtained using a 49 x 49 grid with 66 points on the airfoil. In the actual computational process, a solution was usually first obtained on a 13 x 13 grid with a maximum of 800 relaxation sweeps, then on a 25 x 25 grid with a maximum of 400 cycles, and finally on a 49 x 49 grid with a maximum of 200 iterations. The converged results from the coarser grid are distributed over the next (finer) mesh by interpolation to start the iterations on the next mesh. This grid halving technique accelerates convergence and significantly reduces computational time as demonstrated in Reference 6. The convergence criteria was usually that the maximum change in perturbation potential be less than $1. \times 10^{-5}$. Normally each problem required only about 15 minutes on the IBM 360/65 system or 5 minutes on a CDC 6600 machine.

CONCLUDING REMARKS

A method suitable for analyzing the transonic flow about two-dimensional airfoils has been developed using a stretched Cartesian coordinate system. This method utilizes the full inviscid potential flow equation and exact boundary conditions and solves them via numerical relaxation. A rotated finite difference scheme is employed in order to obtain the correct domain of dependence in supersonic regions; and Jameson's time-like damping is included to ensure numerical stability. In addition, grid halving is used to achieve computational efficiency.

It has been demonstrated by comparison with previous results that it is not necessary to match the computational grid to the airfoil surface and that accurate results can be obtained with the Cartesian grid. Best accuracy is obtained when the mesh size in the leading edge region is nearly square and the order of the leading-edge radius. This accuracy has been demonstrated for both lifting and nonlifting cases at subcritical and supercritical speeds. The program has also been successfully applied to aft-cambered and other airfoils specifically designed for transonic flight.

Texas A&M University
Department of Aerospace Engineering
College Station, Texas

20 November, 1974

REFERENCES

1. Murman, Earll.; and Cole, Julian D.: Calculation of Plane Steady Transonic Flows. AIAA J., Vol. 9, No. 1, Jan. 1971, pp. 114-121.
2. Garabedian, P. R.; and Korn, D. G.: Analysis of Transonic Airfoils. Comm. on Pure and Applied Math., Vol. 24, 1971, pp. 841-851.
3. Steger, J. L.; and Lomax, H.: Transonic Flow about Two Dimensional Airfoils by Relaxation Procedures. AIAA J., Vol. 10, No. 1, Jan. 1972, pp. 49-54.
4. Jameson, A.: Iterative Solution of Transonic Flows over Airfoils and Wings, Including Flows at Mach 1: Comm. on Pure and Applied Math., Vol. 27, 1974, pp. 283-309.
5. South, J. C., Jr.; and Jameson, A.: Relaxation Solutions for Inviscid Axisymmetric Transonic Flow over Blunt or Pointed Bodies. Proc. AIAA Computational Fluid Dynamics Conf., Palm Springs, Calif., July 1973, pp. 8-17.
6. Carlson, L. A.: Transonic Airfoil Design Using Cartesian Coordinates. NASA CR-2577
7. Ludford, G. S. S.: The Behavior at Infinity of the Potential Function of a Two-Dimensional Subsonic Compressible Flow. J. Math. Phys., Vol. 30, No. 3, October 1951, pp. 117-130.
8. Klunker, E. B.: Contribution to Methods for Calculating the Flow about Thin Lifting Wings at Transonic Speeds-Analytic Expressions for the Far Field. NASA TN D-6530, Nov. 1971.
9. Garabedian, P. R.: Estimation of the Relaxation Factor for Small Mesh Size. Math Tables and Aids to Comp., Oct. 1956, pp. 183-185.
10. Lock, R. C.: Test Cases for Numerical Methods in Two-Dimensional Transonic Flows. AGARD Report R-575-70, 1970.
11. Sells, C. C. L.: Plane Subcritical Flow past a Lifting Airfoil. R.A.E. Technical Report 67146, 1967.
12. Whitcomb, R. T.: Review of NASA Supercritical Airfoils. Proc. of the IXth ICAS Congress, Haifa, Israel, Paper No. 74-10, August 1974.

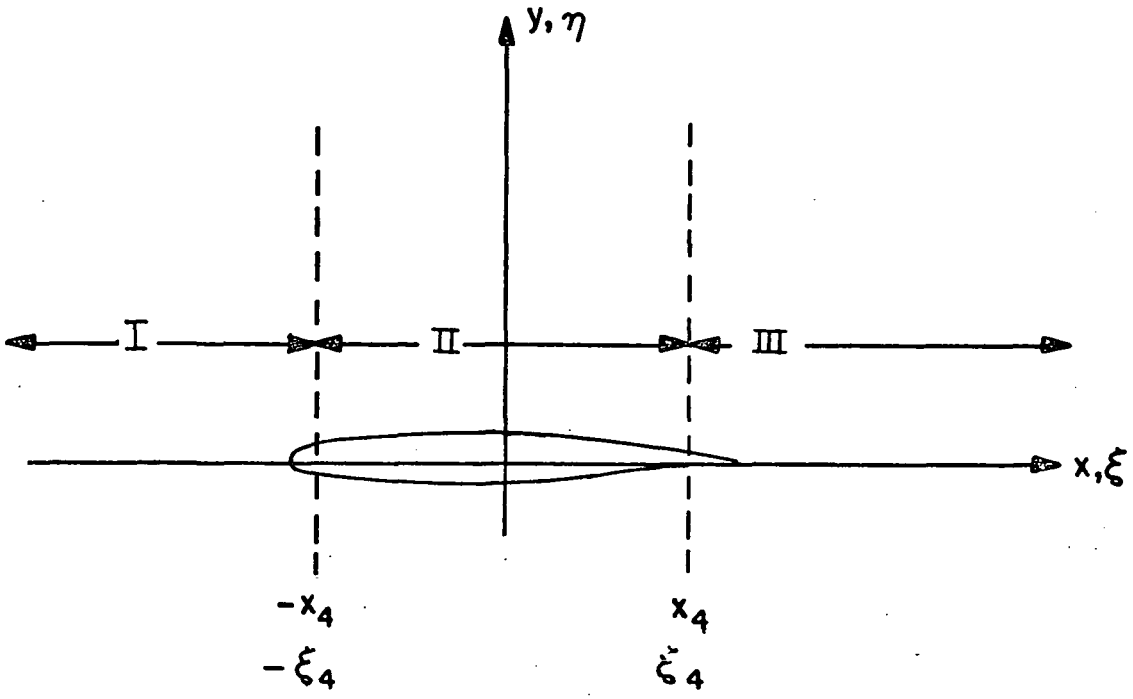

Figure 1--Flowfield Subdivision for Coordinate Stretching

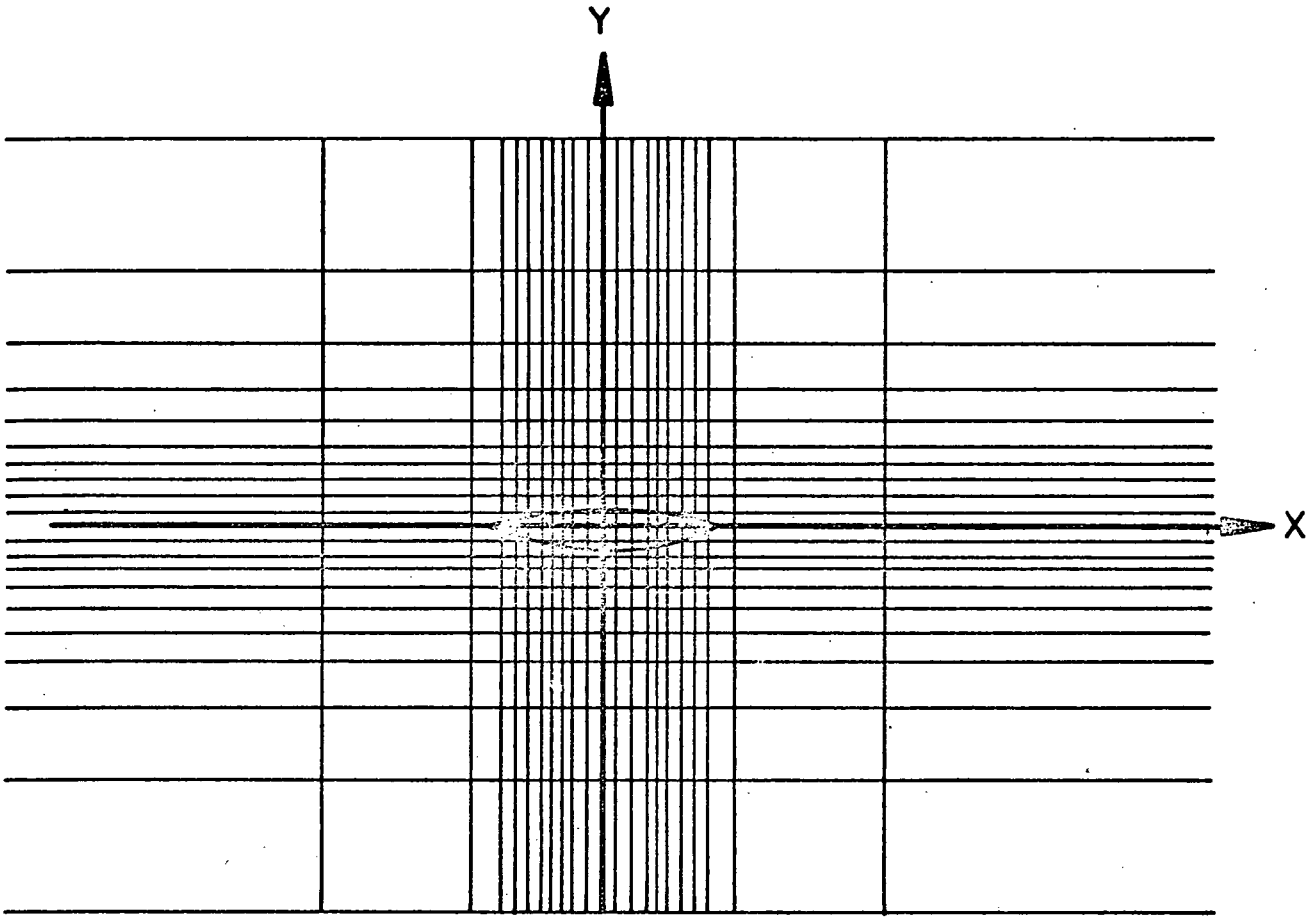

Figure 2--Typical Grid System (25x25)

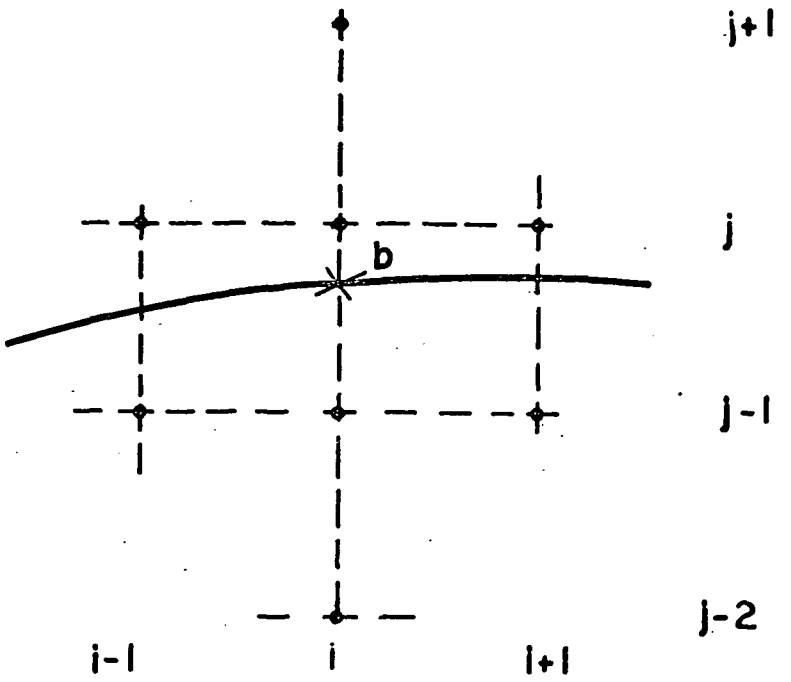

Figure 3--Relationship Between Airfoil and Grid (Upper Surface)

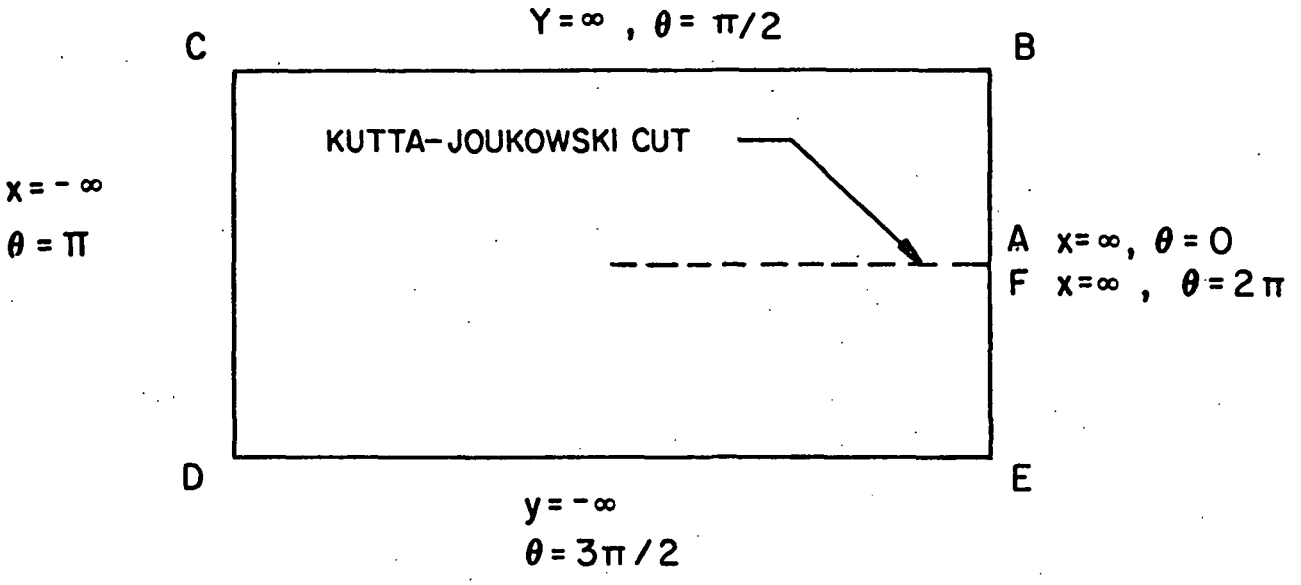

Figure 4--Computational Grid - Infinity Points

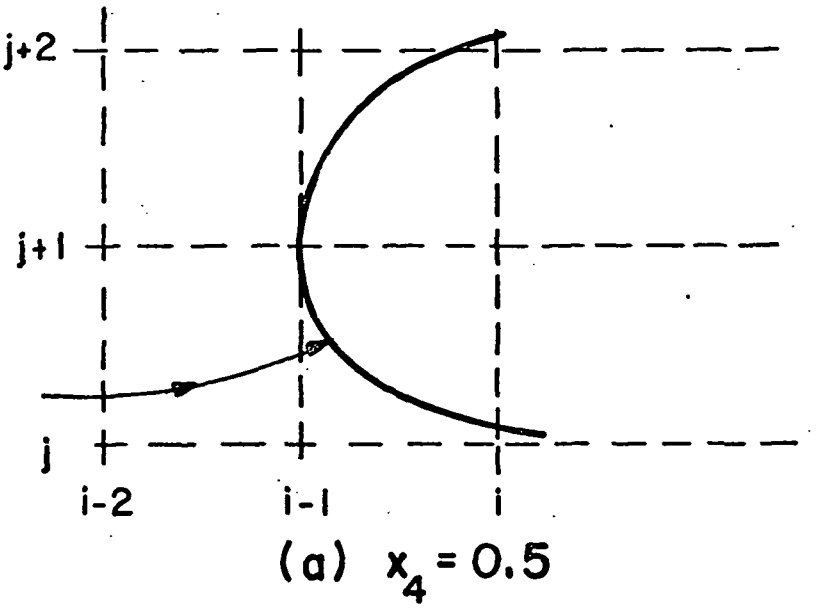

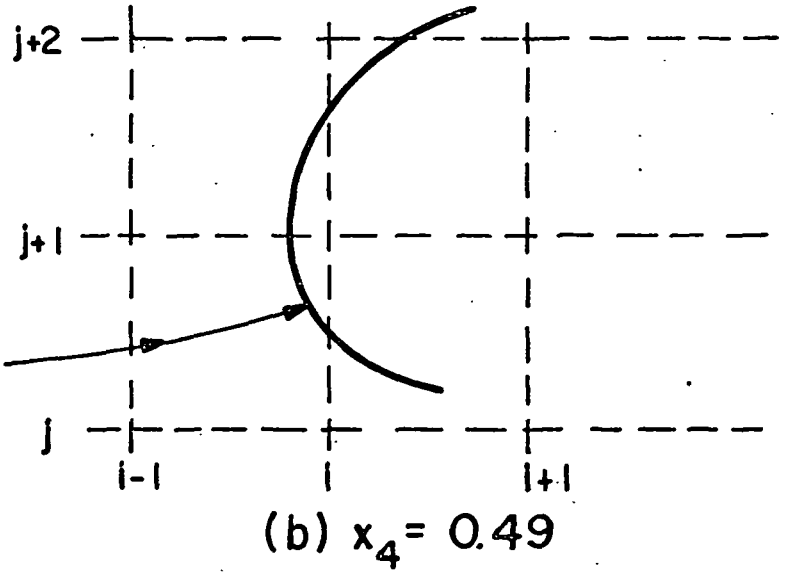

Figure 5--Grid Pattern versus X_4

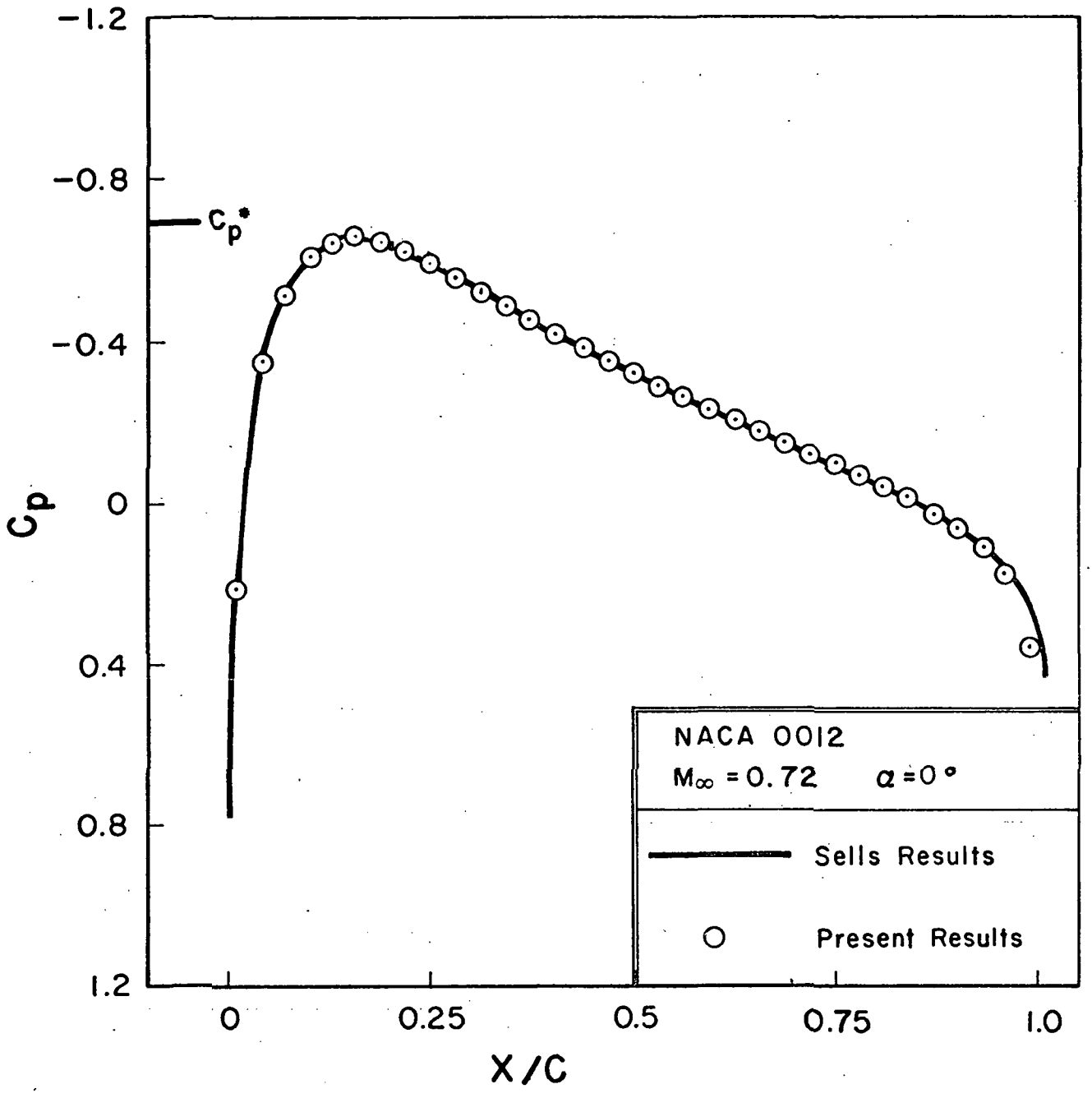

Figure 6--Comparison with Sells for Subcritical Nonlifting Case

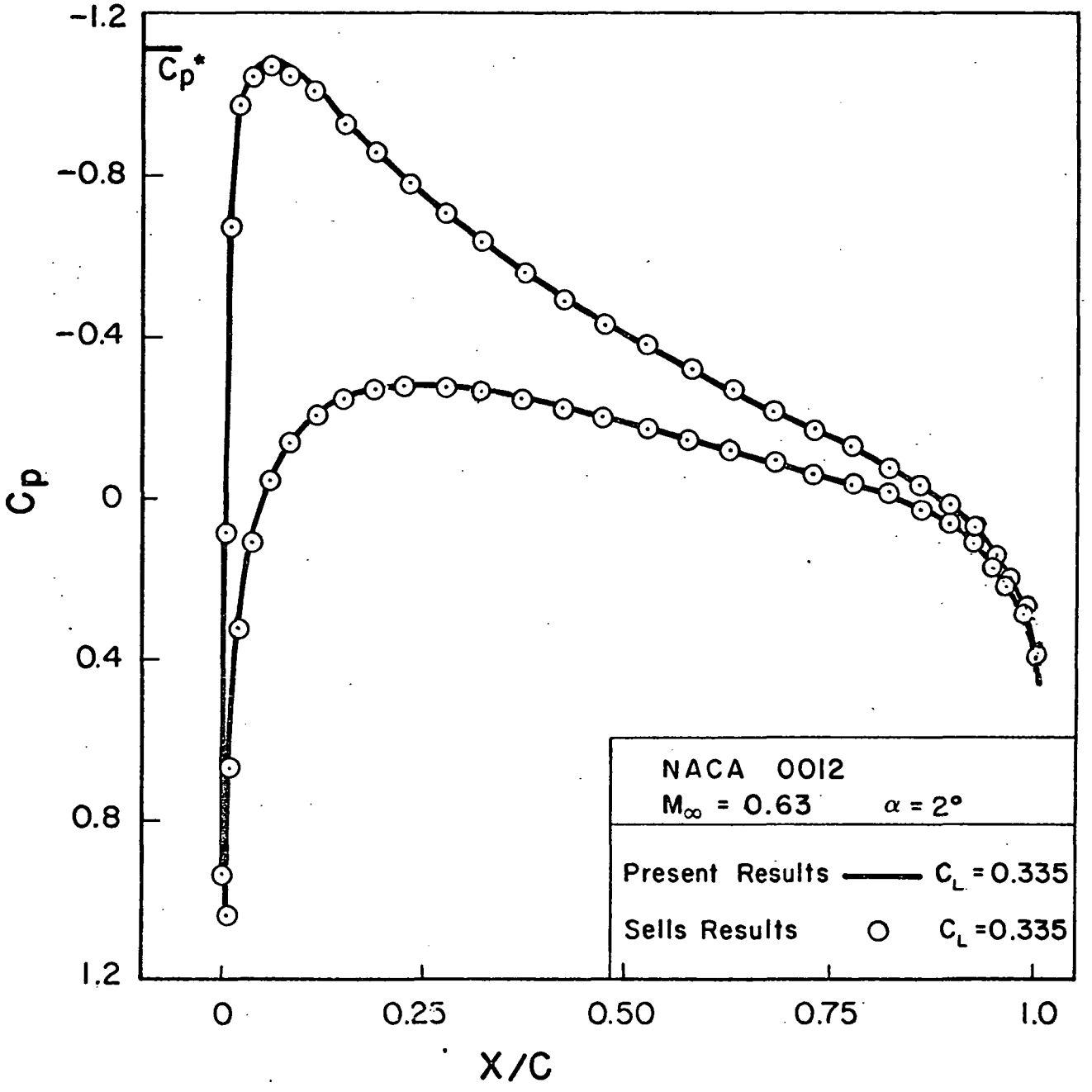

Figure 7--Comparison with Sells for Subcritical Lifting Case

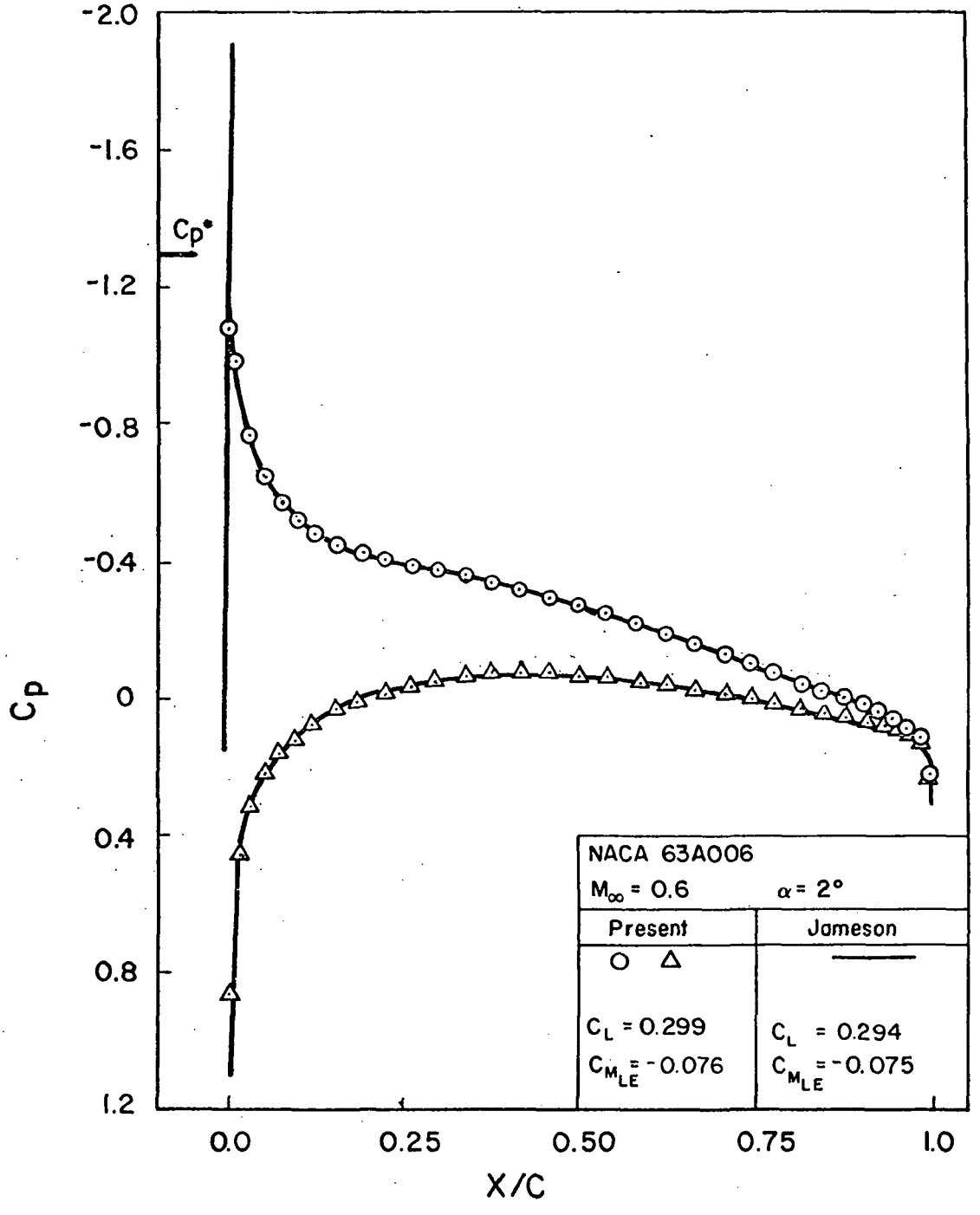

Figure 8--Comparison with Jameson for NACA 63A006

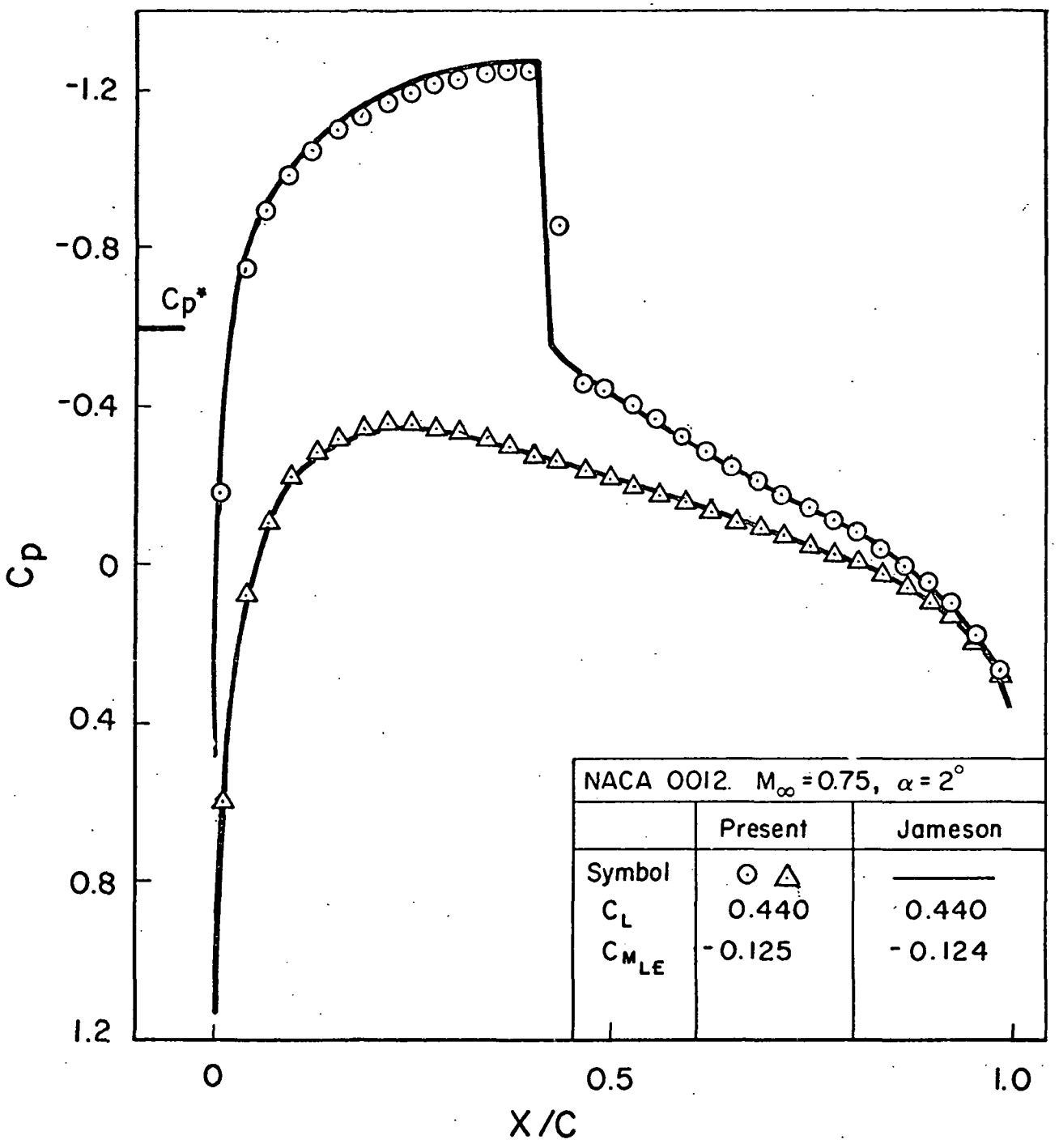

Figure 9--Comparison with Jameson for Supercritical Lifting Case

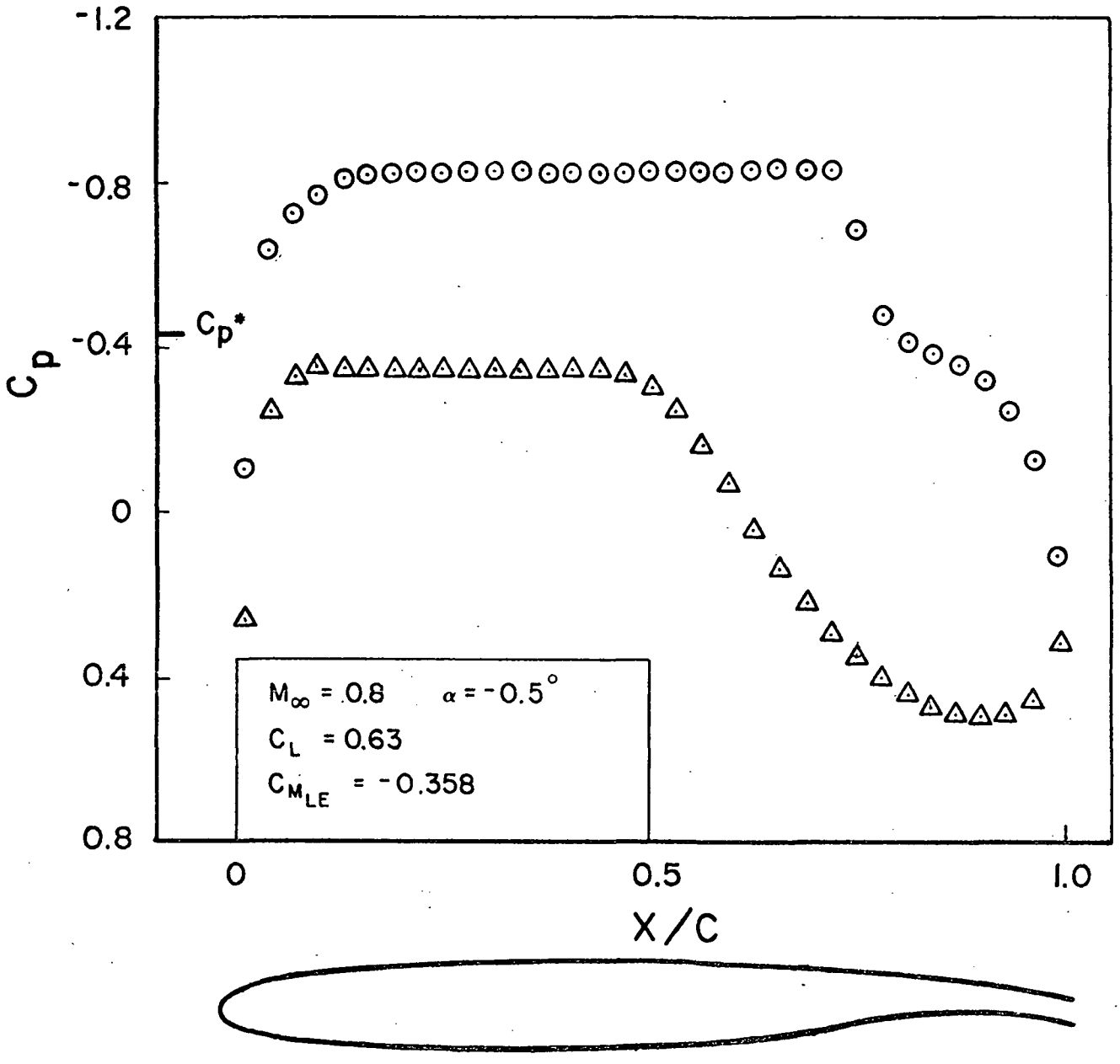

Figure 10--Pressure Distribution for an Aft Cambered Supercritical Airfoil

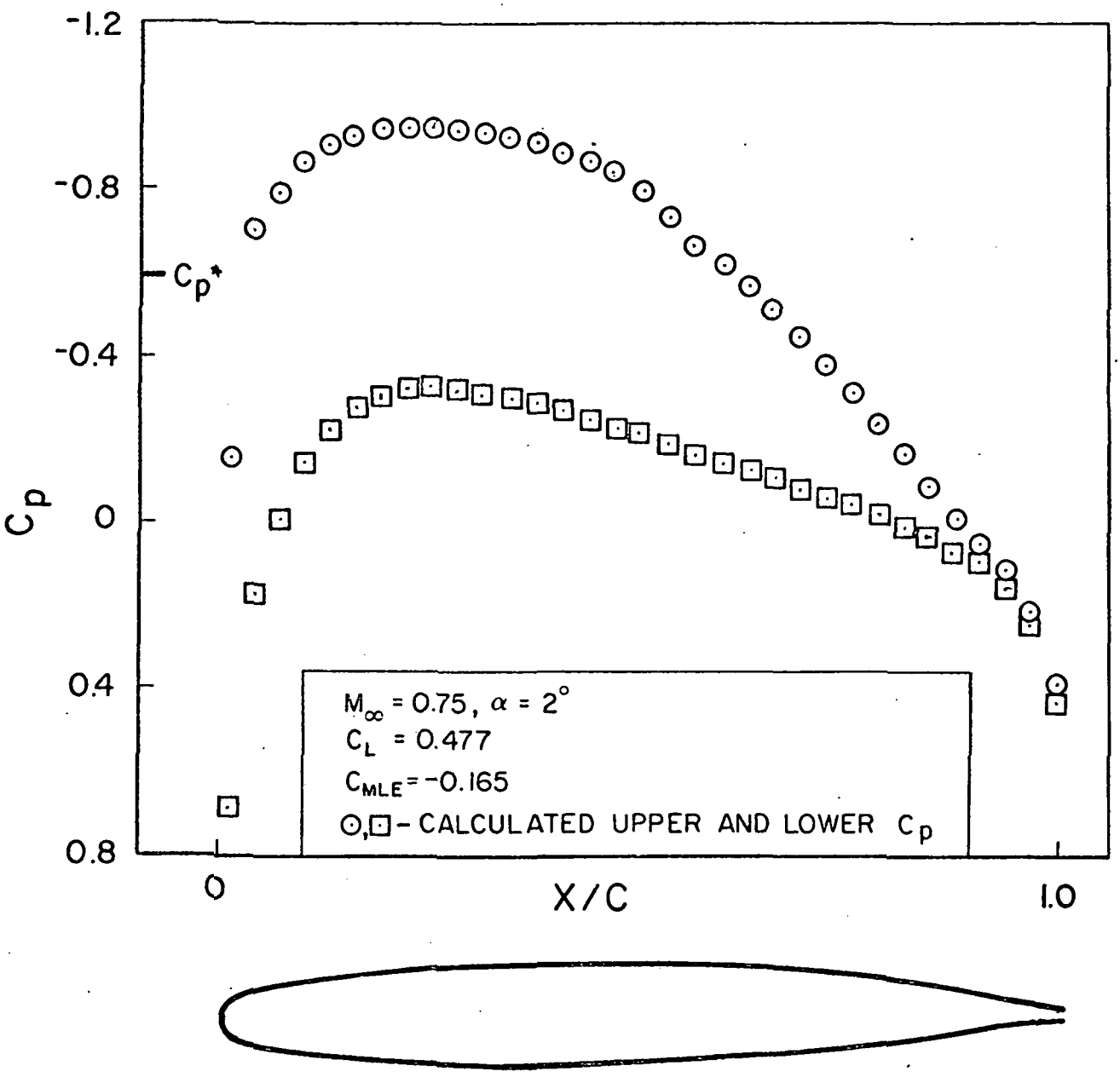

Figure 11--Pressure Distribution for a Supercritical Airfoil

NATIONAL AERONAUTICS AND SPACE ADMINISTRATION
WASHINGTON, D.C. 20546

OFFICIAL BUSINESS
PENALTY FOR PRIVATE USE $300

SPECIAL FOURTH-CLASS RATE BOOK

POSTAGE AND FEES PAID
NATIONAL AERONAUTICS AND SPACE ADMINISTRATION
451

U.S.MAIL

POSTMASTER : If Undeliverable (Section 158 Postal Manual) Do Not Return

"The aeronautical and space activities of the United States shall be conducted so as to contribute . . . to the expansion of human knowledge of phenomena in the atmosphere and space. The Administration shall provide for the widest practicable and appropriate dissemination of information concerning its activities and the results thereof."

—NATIONAL AERONAUTICS AND SPACE ACT OF 1958

NASA SCIENTIFIC AND TECHNICAL PUBLICATIONS

TECHNICAL REPORTS: Scientific and technical information considered important, complete, and a lasting contribution to existing knowledge.

TECHNICAL NOTES: Information less broad in scope but nevertheless of importance as a contribution to existing knowledge.

TECHNICAL MEMORANDUMS: Information receiving limited distribution because of preliminary data, security classification, or other reasons. Also includes conference proceedings with either limited or unlimited distribution.

CONTRACTOR REPORTS: Scientific and technical information generated under a NASA contract or grant and considered an important contribution to existing knowledge.

TECHNICAL TRANSLATIONS: Information published in a foreign language considered to merit NASA distribution in English.

SPECIAL PUBLICATIONS: Information derived from or of value to NASA activities. Publications include final reports of major projects, monographs, data compilations, handbooks, sourcebooks, and special bibliographies.

TECHNOLOGY UTILIZATION PUBLICATIONS: Information on technology used by NASA that may be of particular interest in commercial and other non-aerospace applications. Publications include Tech Briefs, Technology Utilization Reports and Technology Surveys.

Details on the availability of these publications may be obtained from:

SCIENTIFIC AND TECHNICAL INFORMATION OFFICE

NATIONAL AERONAUTICS AND SPACE ADMINISTRATION

Washington, D.C. 20546